

Design and research of Nielsen arch bridge with fully composite structure system

Luojin Cao¹, Nianqin Liu³, Xiangyu Li², Wenming Que³, Yong Li^{1,*}

¹ College of Civil and Transportation Engineering, Shenzhen University, Shenzhen, Guangdong 518060, China

² Shenzhen College of international Education, Shenzhen, Guangdong 518110, China

³ Shenzhen Bridge Design and Research Institute Co., LTD., Shenzhen, Guangdong 518043, China

* Corresponding author: e-mail: Liy2000@163.com

ABSTRACT: China is the kingdom of arch bridges. Based on the principle of structural elastic potential energy standing value, the innovative application of the design theory of composite arch bridge bending and compression is presented, optimize the design of composite structural arch bridge arch axis, and propose the design and construction method of medium-bearing composite Nielsen arch bridge. The design of the medium-bearing composite Nielsen arch bridge is carried out, its structural strength, stiffness and stability are analyzed by finite element analysis. By simulating the parameters of arch axis, sagittal span ratio and arch section, the convergent composite arch axis with solid web foot section is adopted to improve the economic spanning capacity of the composite Nielsen arch bridge and expand the adaptation range of large span arch bridge in plain area or soft base area.

KEY WORDS: fully composite structural system; composite arch bridge; concrete filled steel tube; Nielsen Arch; composite arch axis.

FOR CITATION: Luojin Cao, Nianqin Liu, Xiangyu Li, Wenming Que, Yong Li. Design and research of Nielsen arch bridge with fully composite structure system. *Nanotechnologies in Construction*. 2022; 14(4): 282–293. <https://doi.org/10.15828/2075-8545-2022-14-4-282-293>. – EDN: ICTMEE.

INTRODUCTION

In recent years, with the rapid development of the Belt and Road Initiative and China's infrastructure construction, many heavenly rift valleys have been crossed, in which bridge engineering plays a great role. Arch bridge is one of the main forms of large span bridges, which has the advantages of high strength, large spanning capacity and beautiful shape.

According to the construction form of arch, arch bridges can be divided into deck arch bridge, half through arch bridge and through arch bridge. In terms of materials, it includes steel arch bridge, concrete arch bridge and composite structure arch bridge. Composite structural system arch bridge has the advantages of both steel and concrete arch bridge, and has larger span capacity than traditional arch bridge. When the span of the bridge exceeds 200 m, it is suitable to use the composite structure arch bridge. Composite arch bridge main arch section design, according to domestic and foreign actual bridge data, span diameter in 100 m below the arch rib usually use a single steel pipe section;

span in 100m ~200 m below the arch rib more than 2 steel pipes dumbbell-shaped component section; span in 200m above the use of 4 or more concrete filled steel tube truss section form, the arch rib section often uses variable section form.

1. DESIGN

1.1. Overall Design

A bridge in South China. The city is separated by Qingjiang river, which is 240m wide at the widest point, 175 m wide at the narrowest position and 25 m deep. The location of the bridge was selected according to the development of the city and the surrounding environment. The bridge adopts 210 m span medium-bearing composite Nielsen arch bridge with 25 m width and 1/3.818 sagittal span ratio. The bridge adopts city main road standard, design speed 50 km/h, design load adopts city-A, crowd load 3.5 kN/m, peak acceleration value of ground vibration 0.05 g, bridge seismic measures level 2, design reference period 100 years.

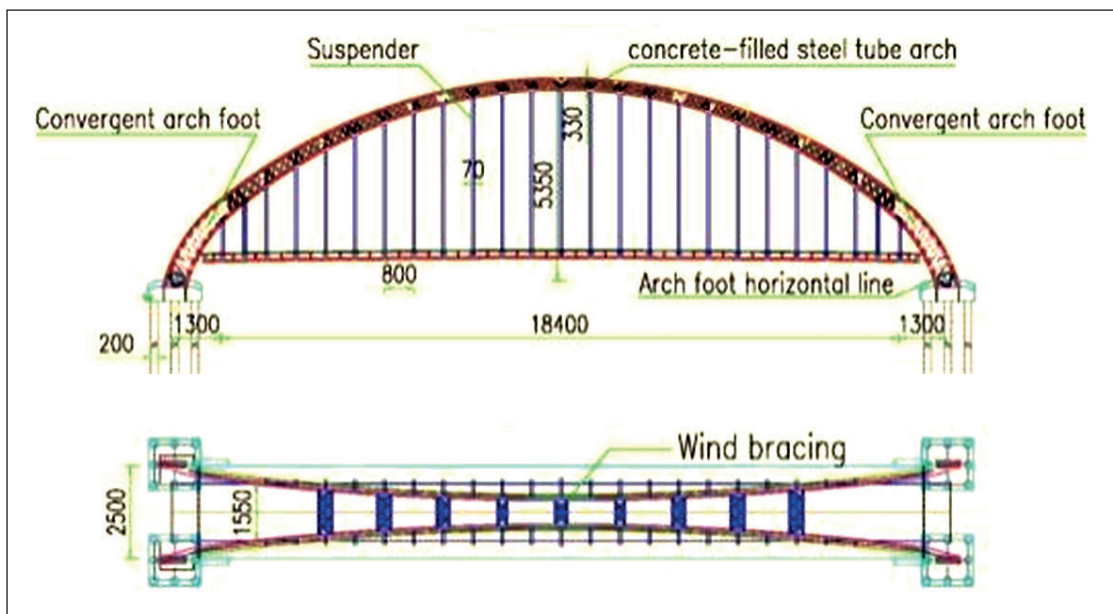


Fig. 1. Fully Composite Structure System Nielsen Arch Bridge

The main arch adopts concrete filled steel tube truss arch with concrete encasement at the foot of the arch. The composite arch axis is composed of suspension chain line and parabolic line, with arch axis coefficient 1.756 and pre-arch degree $L/600$, which is set according to the secondary parabolic line. The main beam adopts wave-truss-slab PC combination beam with a height of 2.2 m.

1.2. Main Arch Design

1.2.1. Main Arch

The arch ribs are 2 pieces of truss Nielsen type arch ribs with 80.707° dip angle, each piece of arch ribs consists of 4 upper and lower chord steel pipes ($\varnothing 900 \times 16$ mm) and upper and lower flat link ($\varnothing 600 \times 12$ mm, double limbs at the boom $\varnothing 600 \times 16$ mm), webbing ($\varnothing 299 \times 10$ mm, webbing at the foot section $\varnothing 351 \times 12$ mm) welded into four limbs lattice truss section, section height from 3.3 m tapered to 6.527 m, width 2.3 m.

C60 self-compacting concrete was pumped in the upper and lower chord main steel pipes and the solid web

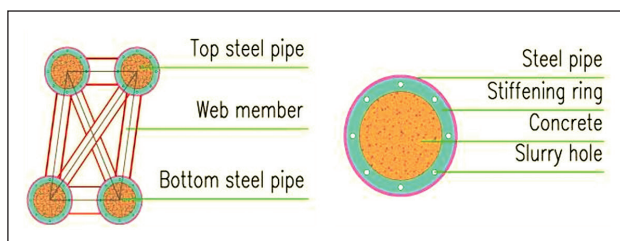


Fig. 2. Arch section form

section of the foot of the arch, with the feeding position at the upper edge of the chord steel pipes in the foot of the arch main steel pipe section. The transverse center distance between the centers of two arch ribs at the top of the arch is 8.0 m, and the transverse center line distance of the foot of the arch is 26 m.

1.2.2. Composite arch axis

The composite Nielsen arch bridge has the advantage of more balanced and reasonable load distribution in the transverse direction compared with the parallel arch bridge. The bridge deck load is transferred to the main arch to realize the redistribution of stress in the main arch, which is a self-balancing structural system and significantly improves the overall stability of the structure.

The arch bridge is a thrust system, by optimizing the arch axis, adopting convergent arch footings, adjusting the inclination of the footing support surface, reducing the horizontal component of the arch axial force, reducing the number of horizontal ties and the workload of cable adjustment.

1) Under the action of constant load, the horizontal thrust generated by the main arch is balanced by horizontal ties and convergent arch footing, thus reducing the horizontal thrust of the arch footing on the foundation of the main arch structure, i.e.

$$H_1 = |H_2 + H_3|, \quad (1)$$

where: H_1 is the horizontal thrust generated by the main arch under the action of constant load; H_2 is the ten-

sion generated by the horizontal ties; H_3 is the horizontal resistance generated by the bearing and pile foundation.

2) Under the action of variable load, the horizontal thrust force generated by the structure is still balanced by the horizontal ties and foundation, i.e.

$$\Delta H_1 = |H'_2 + H'_3|, \quad (2)$$

where: ΔH_1 is the horizontal thrust generated by the main arch under live load; H'_2 is the tension generated by the horizontal ties under live load; H'_3 is the horizontal resistance generated by the bearing and pile foundation under live load.

$$\left(\frac{f_1}{m-1} (chk \xi) = f_2 + \sqrt{x_2 - L_1} \right) \quad (3)$$

$$\left(\frac{kf_1}{m-1} s \square kx = \frac{1}{2\sqrt{x_2 - L_1}} \right) \quad (4)$$

Among them, $\xi = x_1/L_1$; $m = g_y/g_d$; $s \square k\xi = (e^{k\xi} + e^{-k\xi})/2$; $k = ch^{-1}m = \ln(m + \sqrt{m^2 - 1})$.

1.2.3. Transverse coupling system

Bridge arch rib a total of 50 pairs of booms, double boom longitudinal spacing of 8m, double boom spacing of 0.7 m, bridge deck at the boom transverse spacing of 18.5 m boom cable using extruded double HDPE epoxy steel strand finished cable, each boom by 31 \varnothing 15.2 mm epoxy spraying high-strength low loosening, strength level of 1860 MPa prestressed steel hinges, anchor head using high-performance extrusion cold casting anchor, can Adjustable cable force. The inner layer is black, and the outer layer is sky blue.

1.2.4. Stay Cable

Bridge arch rib is a total of 50 pairs of booms, double boom longitudinal spacing of 8m, double boom spacing of 0.7 m, bridge deck at the boom transverse spacing of 18.5 m. boom cable using extruded double HDPE epoxy

steel strand finished cable, each boom by 31 \varnothing 15.2 mm epoxy spraying high-strength low loosening, strength level of 1860 MPa prestressed steel hinges, anchor head using high-performance extrusion cold casting anchor, can Adjustable cable force. The inner layer is black, and the outer layer is sky blue.

1.2.5. Horizontal ties

There are 24 bundles (including 4 spare bundles), 12 high-strength low-relaxation prestressing steel strand bundles on each side, each bundle consists of 19 \varnothing 15.2 mm epoxy steel strands, the standard strength of steel strand fpk = 1860 Mpa, the tied bundle is set in the small steel box tied box at the top of the longitudinal beam, anchored at the cross beam of the arch rib. The bollard strand bundle protects the concrete wire bundle with high-density polyethylene double sheathing, all in black.

1.3. Main Beam Design

1.3.1. Longitudinal Beam

The whole bridge has through-length side longitudinal beam 2 pieces, side longitudinal beam height 2.1 m, side longitudinal beam web for waveform steel web, wavelength is 1000 mm, wave height 200 mm, wave plate thickness is 14 mm, web center spacing 1.3 m, side longitudinal beam lower edge for steel pipe truss composition, lower chord steel pipe with \varnothing 600 \times 12 mm, steel pipe flat link with \varnothing 500 \times 12 mm, longitudinal beam upper edge for through-length steel plate, top plate 2.0 m, thickness of 20mm, two sides of the longitudinal beam center distance of 18.5 m.

1.3.2. Crossbeam

The bridge has 25 crossbeams, crossbeams using triangular steel pipe crossbeam, beam length 25 m, end crossbeam length 29 m, crossbeam longitudinal spacing 8 m,

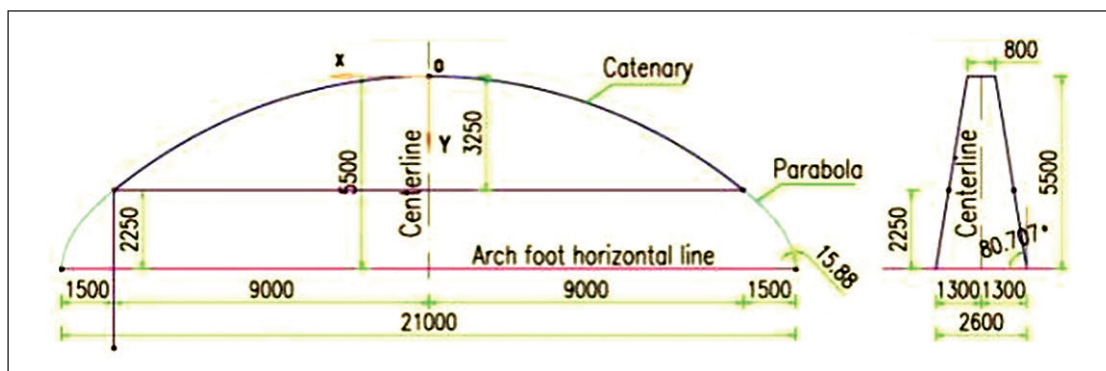


Fig. 3. Suspension chain line + parabolic composite arch axis

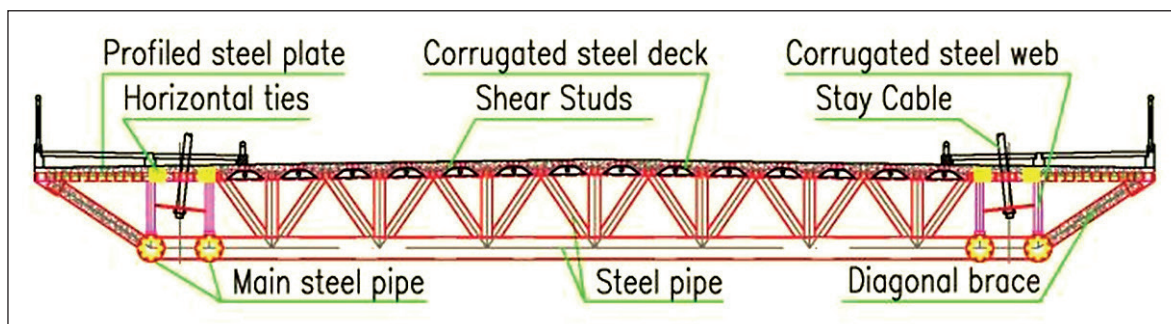


Fig. 4. Deck of wave-truss composite structure

crossbeam lower chord supervisor using $\varnothing 500 \times 14$ mm, by $\varnothing 299 \times 10$ mm web welding into triangular limb lattice truss type section; sidewalk cantilever plate using concrete filled steel tube cantilever brace tube, $\varnothing 299 \times 12$ mm.

2. CALCULATION AND ANALYSIS

Using the calculation results of Midas/civil 2017 calculation software, the model of the whole bridge has a total of 6984 nodes and 12 002 units, the concrete filled steel tube arch ribs and diagonal bracing use SRC combination interface, which is automatically converted to steel by the software according to the strength equivalence principle; the inter-arch support, end crossbeam, main beam lower chord and web are used beam units; the solid web section of the arch foot uses solid units; the boom and horizontal The model adopts the nodal elastic support model pile soil effect, and the corrugated steel webs are simulated by the plate unit. As flat steel webs are used to simulate corrugated steel webs, the effective compressive elastic modulus, flexural elastic modulus and shear modulus of flat steel webs G_{eff} are calculated according to the following formula:

$$G_{eff} = \frac{(b_w + l_w \cos \theta) t_w^2 E_s}{(2b_w^2 l_w + 3b_w^3)(\sin \theta)^2 + t_w^2 b_w + t_w^2 l_w (\cos \theta)^2}$$

$$G_{eff} = \frac{(b_w + d_w) G_w}{b_w + \frac{d_w}{\cos \theta}}$$

According to the formula, E_s is the modulus of elasticity of steel, b_w is the length of flat section of waveform steel web, t_w and l_w are the thickness of waveform steel web and length of inclined plate section, θ is the inclined plate inclination angle, $b_w = l_w \cos \theta$. When the inclination angle of the inclined plate section is greater than 20° , the equivalent flexural modulus of the waveform steel web is close to 0. At this time, the deformation stiffness of the waveform steel web in the axial direction can be ignored. The inclination angle of the inclined plate segments of this bridge is 38.66° , so the effective flexural compressive elastic modulus and flexural elastic modulus are selected

to be 0, and the effective shear elastic modulus $G_{eff} = 6.38 \times 10^4 \text{ N/mm}^2$.

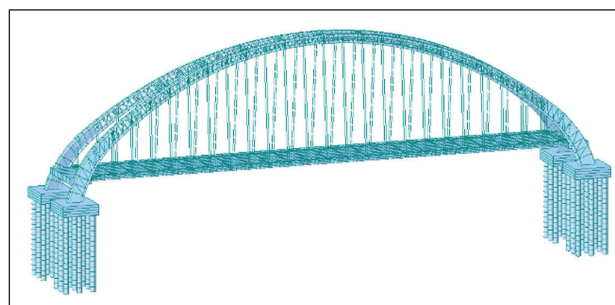


Fig. 5. Composite Nielsen arch bridge finite element model

2.1. Calculated load and boundary conditions

Design load: City-A, transverse arrangement of 6 lanes. Consider span longitudinal discount factor 0.97, live load impact factor is taken as 1.07. Overall temperature load: warming 25 degrees, cooling 20 degrees considered. Local temperature load: temperature gradient of main arch is taken as 8°C , and temperature gradient of main beam is taken as 14°C . The base displacement is 100mm vertical displacement and 6mm horizontal displacement of the support. each load combination is as follows: 1) combination 1: (basic combination 1): $1.1 \times (1.2 \text{ constant load} + 1.4 \text{ live load} + 0.825 \text{ wind load} + 1.05 \text{ overall warming} + 0.5 \text{ uneven settlement})$; 2) combination 2: (basic combination 2): $1.1 \times (1.2 \text{ constant load} + 1.4 \text{ live load} + 0.825 \text{ wind load} + 1.05 \text{ overall cooling} + 0.5 \text{ uneven settlement})$; 3) combination 3: (standard combination 1): 1 constant load + 1 live load + 1 wind load + 1 overall warming + 1 uneven settlement; 4) combination 4: (standard combination 2): 1 constant load + 1 live load + 1 wind load + 1 overall cooling + 1 uneven settlement.

Boundary conditions: the pile foundation is rigidly connected to the bearing platform; the pile foundation is elastically supported by nodes with the foundation, and the spring stiffness is calculated by the M method; the

mid-span main beam is connected to the crossbeam bull leg by springs.

2.2. Static force analysis

2.2.1. Structural strength

According to the finite element analysis results, the arch axis consists of the middle section suspension chain line and the two ends parabolic line, the middle section is mainly in the form of arch pressure, the two ends are closer to the form of rigid frame structure force, constant load thrust can be balanced by the ties. The composite stresses of the arch rib steel members under the basic combination are in the range of $-26.2\text{MPa}\sim 192.5\text{MPa}$, and the composite stresses of the main beam are in the range of $-185.3\text{MPa}\sim 222.4\text{MPa}$, which meet the code requirements.

2.2.2. Structural stiffness

The structural stiffness (normal use limit state) is verified by standard combination, and the displacement envelope under the most unfavorable load combination of the whole bridge is shown in Fig. 6. The maximum vertical displacement of the main beam is 123.5 mm in the middle of the span, which is $1/1700 < 1/800$ of the span, meeting the specification requirements.

2.2.3. Analysis of convergent arch footing test

In order to study the influence of convergent arch footing on horizontal thrust, the analysis is calculated according to tensioned horizontal ties and untensioned horizontal ties respectively, the maximum horizontal thrust of main arch footing is 63856 kN. the maximum shear force of untensioned horizontal ties is 20,167 KN, the maxi-

Table 1

Summary of stress calculation results

Section	Group 1 (MPa)	Group 2 (MPa)	Group 3 (MPa)	Group 4 (MPa)
Maximum stress of on main arch	142.4	128.6	153.5	137.2
Maximum stress of arch rib under main arch	177.7	165.2	193.5	181.3
Main arch horizontal joint maximum stress	168.3	151.2	147.8	133.9
Maximum stress of main arch belly bar	192.5	201.5	188.5	191.7
Maximum stress of concrete in arch	-26.2	-25.1	-23.8	-23.5
Maximum wind support stress	-162.2	-151.8	-143.1	-133.7
Maximum stress of main girder chord	211.5	222.4	198.8	173.2
Maximum stress of web of main girder	160.7	166.6	143.2	138.7

Table 2

Summary of calculation results of internal force of arch foot

State	Longitudinal bridge thrust (kN)	Vertical force (kN)	Bending moment in arch surface (kN·m)	Torque (kN·m)
Constant load	8178.3	36483.2	-42395.6	-6005.9
Crowd load	1467.1	-1292.4	-11060.3	-1810.1
heating	455.7	1.6	-21029.5	-5337.4
cooling	-915.4	-1.4	22202.6	5291.8
Lane load max	2348.1	56.4	16846.3	2595.4
Lane load min	-81.4	-2037.9	-32051.3	-5102.4
Settlement max	0.1	4.7	562.1	86.2
Settlement min	-0.3	-4.7	-555.0	-84.8
Basic combination max	18011.9	33711.1	37631.6	8506.4
Basic combination min	4833.7	50492.5	-174764.8	27891.6

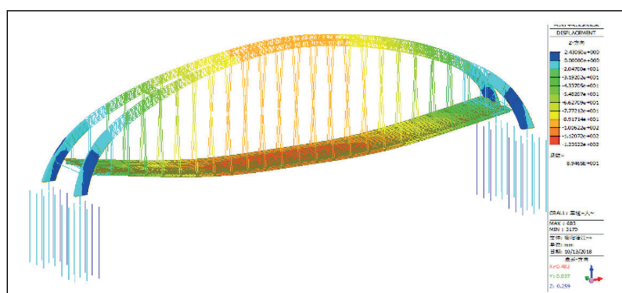


Fig. 6. Displacement under the most unfavorable load

imum bending moment is 210680 KNm, the maximum shear force after tensioned horizontal ties ($0.4R_y \cdot b$) is 14688 KN, the maximum bending moment 104777 KNm, a reduction of 50.3%.

2.2.4. Foundation Displacement and Temperature Response

By calculating combination 3 and combination 4 separately, the effects of foundation dislocation and temperature action on the structure are analyzed. The study shows that compared with load combination 1, the arch rib stress increases by 5.3% when the support is unevenly settled by 100 mm; the arch rib stress increases by 0.38% when the support is horizontally displaced by 6mm; and the arch rib stress increases by 11.9% when the temperature decreases by 20°C.

2.2.5. Fatigue Assessment

According to (Code for design of highway steel structure bridges) (JTGD64-2015) Article 5.5.2, carry out checking calculation adopt calculation model I, concentrated load is 0.7 Pk, the uniformly distributed load is 0.3 qk. Then, under fatigue load, as shown in Figure 3.16, the maximum stress amplitude of the main beam is: $38.8 + 21.3 = 59.1$ MPa. According to Appendix C Fatigue details table C.0.5 of the (Code for design of highway steel structure bridges): Butt weld fatigue detail category $\Delta\sigma_c = 100$ MPa, $\Delta\sigma_d = 0.737$, $\Delta\sigma = 0.737 \times 100 = 73.7$ MPa, ac-

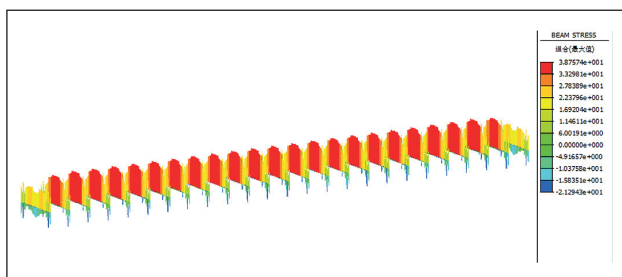


Fig. 7. Normal stress envelope under the most unfavorable fatigue load combination of the whole bridge

ording to the calculation results, the fatigue stress amplitude is less than the allowable value, which meets the design requirements.

2.3. Checking calculation of bearing platform and arch seat

The known cushion cap is 4 m high, 14.6 m wide, arch seat height 1.5 m, pile spacing 2 m, since the distance between piles is less than 3 times the pile diameter, therefore, the full width of the cushion cap is taken as the calculated width of the cushion cap. The distance between the center of the pile and the edge of the arch seat is less than the height of the pile cap, according to the specification, the bearing capacity is checked according to the tension and compression bar model method.

$$\theta_1 = \tan^{-1} [h_0 / (a + x_1)].$$

In the formula θ_1 is the included angle between the inclined compression rod and the pull rod h_0 is the effective height of bearing platform (mm), a is the distance from the intersection of the center line of the compression bar and the top surface of the bearing platform to the edge of the pier and abutment, Let $a = 0.15h_0$, x_1 is the distance from the pile center to the edge of pier and abutment.

$$\gamma_0 C_{i,d} \leq t b_s f_{ce,d}$$

$$f_{ce,d} = \frac{\beta_c f_{cd}}{0.8 + 170 \varepsilon_1} \leq 0.85 \beta_c f_{cd}$$

$$\varepsilon_1 = \frac{T_{i,d}}{A_s E_s} + \left(\frac{T_{i,d}}{A_s E_s} + 0.002 \right) \cot^2 \theta_1$$

$$t = b \sin \theta_1 + h_a \cos \theta_1$$

$$h_a = s + 6d$$

In the formula γ_0 is the important coefficient of bridge structure $C_{i,d}$ is the design value of the internal force of the compression bar; $f_{ce,d}$ is the design value of equivalent compressive strength of concrete compression bar $T_{i,d}$ is the design value of the internal force of the tie rod β_c is the relevant parameter of concrete strength grade f_{cd} is the design value of concrete axial compressive strength A_s is the area of tie bar reinforcement within the calculated width of bearing platform E_s is the elastic modulus of reinforcement.

According to the calculation, $\gamma_0 C_{i,d} = 52225$ kN < $t b_s f_{ce,d} = 358341$ kN, Meet the specification requirements.

2.4. Structural stability

The wind stability is a problem of large span arch bridge. The stability analysis considers the loads, the moving load is arranged according to the most unfavorable

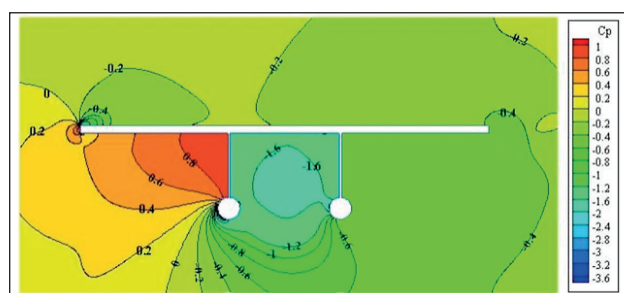


Fig. 8. Average wind pressure distribution

working condition of the arch foot axial force, the design wind speed is 27.2 m/s (10m high from the ground, 1% frequency, 10 min average maximum wind speed value), and the wind resistance coefficient of the single arch rib section is 1.4.

The structural stability calculation of this bridge is carried out by the spatial finite element method. Calculation, respectively, in the bridge deck applied live load, the stability safety factor K of the structure is defined as P_{cr}/PT , where P_{cr} is the ultimate bearing capacity of the structure, PT in the bridge state for the structure of the self-weight and the sum of the operating live load, in fact K is the structure to reach the ultimate bearing capacity about the PT loading multiplier.

Table 3
Arch bridge structure flexural stability characteristic value

Mode	Critical load factor	Working condition	Unstable mode
Mode 1	6.8	Constant load variable Other constant	Longitudinal asymmetry
Mode 2	8.2		Longitudinal symmetry
Mode 3	11.4		Symmetric distortion
Mode 1	36.7	Variable live load Other constant	Longitudinal asymmetry
Mode 2	43.0		Longitudinal symmetry
Mode 3	60.9		Symmetric distortion

Table 4
Dynamic characteristics analysis results

Vibration order	Period (s)	Frequency (Hz)	Description of key vibration characteristics
1	2.368	0.422	Arch rib transverse bend
2	1.648	0.607	Second-order vertical bend of arch beam
3	1.561	0.641	Arch rib second order transverse bend
4	1.150	0.870	Second-order symmetrical vertical bending of arch beam
5	1.001	0.992	Main beam first-order transverse bend
6	0.918	1.090	Third-order transverse bend of arch rib
7	0.716	1.397	Second order torsion of arch beam
8	0.648	1.546	Third-order torsion of arch beam

2.5. Structural dynamic response

The dynamic characteristics of the structure were analyzed, and the structural fundamental frequency was 0.422 Hz. The first-order frequency range of the pedestrian pace: 1.6~2.4 Hz in the vertical direction, and half of 0.6~1.2 Hz in the lateral direction, which is recommended by the European British Standard BS5400 and the German Standard to avoid the lateral vibration frequency of 0.5~1.2 Hz. According to the calculation results, this bridge is far from the possible resonance zone.

3. CONSTRUCTION

3.1. Construction scheme

The structure can be constructed by cable tower crane. This scheme can reduce the bridge construction risk and the stress change of the arch bridge during construction. Specific construction steps are as follows.

- 1) Foundation construction – foundation inspection and acceptance – erection of tower – buckling, sling and cable installation.
- 2) Steel structure factory acceptance – transportation of arch rib segments – assembly of arch rib segments.

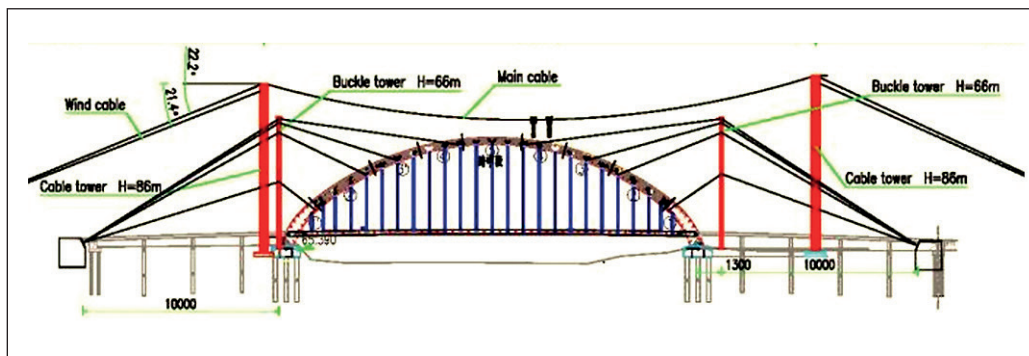


Fig. 9. Construction layout of cable tower crane

3) Lifting arch ribs section by section – tensioning temporary horizontal ties in batches – monitoring and surveillance – main arch alignment adjustment – closing and welding of main arch (final welding of arch foot and pre-buried steel plates) – main arch alignment acceptance.

4) Pumping C60 self-compacting concrete concrete filled steel tube – monitoring deformation of the main arch – detecting compactness and voids – epoxy resin patching to compactness – acceptance of the main arch.

5) Sling hanging longitudinal beam – longitudinal beam joint – through the vertical sling, progressive adjustment of the bridge deck line shape, so that the sling force is uniform, while the bridge deck line shape to meet the specification requirements; horizontal tie tension is large, should pay attention to the radial force generated by the vertical curve of the tie, should be attached to a certain lateral support.

6) Sling suspension crossbeam – crossbeam joints – batch tensioning temporary and permanent horizontal ties – adjust the deck alignment.

7) Cast-in-place bridge deck slab – laying bridge deck pavement – tensioning permanent horizontal ties in batches and symmetrically loosening the temporary horizontal ties.

8) Each construction stage needs to be in accordance with the loading procedure chart and monitoring data synchronous adjustment of the boom cable force, horizontal ties cable force.

9) In accordance with the city and highway bridge inspection specification requirements, static load, dynamic load test, completion acceptance.

3.2. Cable tower crane

The cable crane is composed of rope system, tower system, anchoring system, cable wind system, mechanical and electrical system, etc. When the site conditions are suitable, the cable tower and buckling tower are designed separately. The span of the cable crane covers the engineering lifting operation of the whole bridge. The whole bridge has 2 cable towers and 4 buckling towers. Buckle

crane is separated, arch first and then beam, from side to middle, symmetrical installation.

3.3. Construction process analysis

The construction phase simulation analysis was carried out by Midas space program.

This calculation assumes that the arch ribs are assembled throughout the process and requires that for each section of arch ribs lifted, the tension of all buckling cables is adjusted during the unloading process of the main cables to ensure that all forces are uniform. When lifting each section of arch ribs, adjust the buckling cable tension corresponding to the section of arch ribs so that it can turn slightly near the design arch axis and the coordinates of the lifting point reach the predetermined height, and then fix the front end of the rib section with the last arch rib; when the whole arch ribs are pre-closed, readjust all the buckling cable tension so that the actual arch axis is as close as possible to the theoretical arch axis, requiring an error of ≤ 5 mm.

To simplify the calculation process, the following assumptions are made: During the erection of the arch ribs, the foot of the arch is equipped with a rotating hinge and no additional bending moment is generated; The stiffness of each arch rib section is infinite with respect to the buckling cable and is regarded as a rigid body; It is assumed that the center of gravity of each arch rib section is located in the center of the longitudinal section; The influence of the wind cable on the buckling cable tension is not considered; The force generated by the closing section is borne by half of the buckling cable on each bank.

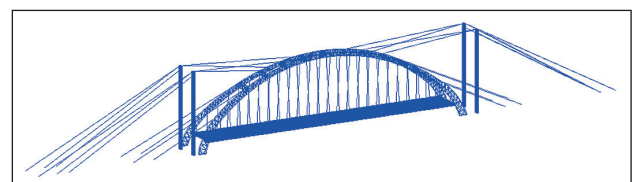


Fig. 10. Construction calculation model

Table 5
South shore snapping rope force change (kN)

	Withhold 1 (kN)	Withhold 2 (kN)	Withhold 3 (kN)	Withhold 4 (kN)
Section 1	254.3			
Section 2	275.9	402.0		
Section 3	262.6	394.6	769.5	
Section 4	235.0	374.7	637.5	1057.6
Section 5 (Closing section)	211.6	359.5	590.4	1068.3
Concrete	152.8	330.6	594.1	1092.9
Maximum cable force	275.9	402.0	769.5	1092.9
Vibration influence Factor 1.1	303.5	442.2	846.5	1202.2
Safety factor	6.02	4.13	4.32	3.04

Table 6
North shore snapping rope force change (kN)

	Withhold 1 (kN)	Withhold 2 (kN)	Withhold 3 (kN)	Withhold 4 (kN)
Section 1	253.4			
Section 2	274.5	433.8		
Section 3	260.7	425.7	787.0	
Section 4	232.7	405.4	667.7	1054.8
Section 5 (Closing section)	209.1	389.9	624.1	1062.8
Concrete	150.7	359.9	624.8	1084.4
Maximum cable force	274.5	433.8	787.0	1084.4
Vibration influence Factor 1.1	302.0	477.2	865.7	1192.8
Safety factor	6.05	3.83	4.22	3.06

The calculation shows that the maximum vertical displacement of the main arch during the construction phase is 156.6 mm, which is $L/1341$ and meets the requirements of the construction specification.

4. CONCLUSION

According to the design and research of the composite Nielsen arch bridge, composite with the analysis of various technical indicators, we can draw the following conclusions.

1) The arch axis consists of the suspension chain line in the middle section and the parabolic line at both ends, the arch axis and pressure line are partially deviated at the foot of the arch, the middle section is dominated by the pressure form of the arch, the two ends are closer to the rigid frame structure form of force, the overall scheme of the structure is reasonable.

2) Composite structure system Nielsen arch bridge is a thrust system, which has strong adaptability to geological conditions. Under the action of constant load, by adopting convergent arch footing, the horizontal thrust of arch

Table 7

Vertical displacement of each observation point of the main arch during construction (mm)

			1	2	3	4	5	Filled steel pipe
South Shore	G1	Displacement increment	-0.3	-8.6	3.3	8.1	7.0	15.7
		Cumulative displacement	-0.3	-8.9	-5.5	2.6	9.6	25.3
	G2	Displacement increment		-52.9	-0.8	20.0	12.4	-8.0
		Cumulative displacement		-52.9	-53.7	-33.7	-21.3	-29.3
	G3	Displacement increment			-0.3	10.3	-13.0	-49.5
		Cumulative displacement			-0.3	10.1	-3.0	-52.5
	G4	Displacement increment				0.5	-51.4	-79.4
		Cumulative displacement				0.5	-50.9	-130.3
North Shore	G5	Displacement increment	-0.3	-8.5	3.5	8.3	7.0	15.7
		Cumulative displacement	-0.3	-8.7	-5.3	3.0	10.0	25.7
	G6	Displacement increment		-52.9	-0.5	20.6	12.7	-8.2
		Cumulative displacement		-52.9	-53.4	-32.8	-20.1	-28.3
	G7	Displacement increment			0.0	10.8	-12.8	-49.7
		Cumulative displacement			0.0	10.8	-2.0	-51.7
	G8	Displacement increment				0.0	-51.2	-79.6
		Cumulative displacement				0.0	-51.3	-130.8
Closing section	G9	Displacement increment					-67.7	-88.8
		Cumulative displacement					-67.7	-156.6

footing is effectively reduced by 35.9%, which obviously saves the horizontal ties and engineering cost.

3) In order to give all by play to the mechanical properties of the steel-concrete composite material in both tension and compression, based on the principle of the standing value of the elastic potential energy of the structure, the convergent asymptotic curvature of the main arch axis in the foot section, the first-order derivative

continuity condition of the suspension chain line and parabolic line in the arch axis at the transition point are innovatively proposed, and the composite arch axis general equation of the composite structure arch bridge is established to reduce the horizontal thrust of the main arch, improve the lateral stability, reduce the project cost, and improve the economic spanning capacity of the large span composite structure arch bridge is improved.

REFERENCES

1. Cai Shaohuai. The latest development of concrete filled steel tubular structure technology in China. *Journal of Civil Engineering*. 1999; 32(4): 16–26.
2. Fang Qinhan. Whhu Changjiang Bridge. *Journal of Huazhong University of science and technology (Urban Science Edition)*. 2000; 19: 1–4.
3. Qin Qhunquan. Construction technology of cable-stayed bridge with plate truss composite structure of Wuhu Changjiang Bridge. *Journal of Civil Engineering*. 2005; 38(9): 94–98.
4. Zhu Hongping, Tang Jiayang. Three-dimensional finite element model for dynamic analysis of cable-stayed bridge. *Journal of Vibration Engineering*. 1998; 12(1) 85–89.
5. Li Yong. *Theory and application of long-span steel-concrete composite bridge*. Science Press; 2013.
6. Li Yong. *Wave truss composite structure bridge*. Science Press; 2015.

7. Zhu Shi-Feng. *Study of Geometric Shape Control and Closure Techniques of Multi-Span Continuous Rigid-Frame Bridge Structure* (Master Dissertation). Chongqing: Chongqing Jiaotong University; 2008.
8. Liu Yuqing. *Composite structure bridge*. Beijing: China communication press; 2005.
9. Cai Shaohuai. *Code for design and construction of concrete filled steel tubular structures*. Beijing: China Planning Press; 1992.
10. Jin Chengdi. *Prestressed concrete beam arch composite bridge – Design Research and Practice*. Beijing: China communication press; 2001.
11. Liu Chang-Guo, Yin Canbin. Analysis and Experimental Study on Jacking Force for High Temperature Closure of Con-rinuuous Rigid-Frame Bridge. *Highway Engineering*. 2009; (10): 83–86.
12. Yin Can-bin, Wang Jie-jun, Tang Can. Algorithms for the Jacking Force of High-Temperature Closure of a Continuous Rigid-Frame Bridge. *Journal of Central South University of Forestry&Technology*. 2009; (1): 111–116.
13. Chen Yiyan. *Design and construction of prestressed concrete bridge with corrugated steel webs*. Beijing: China communication press; 2009.
14. Zhou Qijing. *Design and Construction Manual of steel-concrete composite structure*. Beijing: China Architecture& Building Press; 1991.
15. Nie Jianguo. *Principle and example of steel-concrete composite structure*. Beijing: Science Press; 2009.
16. Chen Baochun. *Design and construction of concrete filled steel tubular arch bridge*. Beijing: China communication press; 2002.
17. Yi Shujun. Design of (88+160+88) m self anchored deck arch bridge over Shanghai Hangzhou Expressway on Shanghai Hangzhou Passenger Dedicated Line. *Railway Standard Design*. 2010; (5): 57–60.
18. Li Yong. *Research on space theory and application of long-span steel-concrete composite bridge*. Doctoral thesis of Huazhong University of science and technology; 2011.
19. Zhang Lianyan, Li Zhesheng, Cheng Maofang. *Concrete filled steel tubular space truss composite beam structure*. Beijing: China communication press; 2001.
20. Hui Zhou, Liu Zhao, Huang Xiaodong. Optimal design of three span deck prestressed concrete arch bridge. *Southeast University Newspaper*. 2007; (2): 296–300.
21. Xv Yong, Ma Tinglin, Chen Kejian. *Design of concrete filled steel tubular arch of Beipanjiang bridge on Shuibai Railway*. Beijing: China Railway Science; 2003.
22. Lin Tongyan, Burns Ned H. *Prestressed concrete structure design*. Beijing: China Railway Publishing House; 1983.
23. Chen Zhaoyuan, Zhao Guopan. *Guide for durability design and construction of concrete structures*. Beijing: China Construction Industry Press; 2004.
24. Zhou Nianxian. *Comparison and selection of bridge schemes*. Version 2. Shanghai: Tongji University Press; 1997.
25. He Pizhuang. *Bridge aesthetics*. Beijing: China communication press; 1999.
26. Chen Baochun, Sun Chao, Chen Youjie. Application and development of bridge Swivel Construction Method in China. *Highway transportation technology*. 2001; (2): 24–28.
27. Zhang Lianyan, Cheng Maofang, Tan Bangming. *Bridge Swivel Construction*. Beijing: China communication press; 2002.
28. Huang Qingwei, Chen Baochun. Design and construction of maegu bridge in Japan. *Fujian architecture*. 2005; (1): 58–62.
29. Zou Yi-song, Shan Rong-Siang. The Determination of Jacking Force for Closure of Continuous Rigid Frame Bridge. *Journal of Chongqing Jiaotong Institute*. 2006; (2): 12–15.
30. Gu Anbang. *Bridge Engineering (upper and lower)*. China communication pres; 2000.
31. Li Yong, Chen Yiyan, Nie Jianguo, Chen Baochun. *Design and application of steel-concrete composite bridge*. Science Press; 2002. Version 1.
32. Fan Lichu. *Bridge Engineering (Volume II)*. China communication press; 2001.
33. Li Shuqin, Sun Tianming. Research on calculation method of PBL shear members in steel-concrete composite box girder. *Highway*. 2010; 15(08): 64–66.
34. Zhou Keming, Li Xia. Cantilever truss structure under lateral force. *Engineering Mechanics*. 2007; 24(10): 66–40.
35. He Minjun. Design and construction of horizontal cable for continuous steel truss arch double cantilever erection. *Transportation Technology*. 2006; 26(1): 62–65.
36. Zhong Shantong. *Prestressed steel structure*. Harbin: Harbin Institute of Technology Press; 1986.
37. Li Chuanxi, Xia Guiyun. Summary of static analysis of stay cable. *Central South Highway Project*. 2001; 2.
38. Hua Xiaoliang. *Nonlinear analysis of bridge structure*. Beijing: China communication press; 1997.
39. Liu Guangdong, Wang Jiejun. Decomposition form of geometric stiffness matrix of spatial beam element. *Journal of Hunan University*. 1992; 1.

THE STUDY OF THE PROPERTIES OF NANOMATERIALS

40. Zhao Chao. *Principle of structural matrix analysis*. Beijing: People's Education Pres; 1982.
41. Meng Fanzhong. *Elastoplastic finite deformation theory and finite element method*. Beijing: Tsinghua university press; 1985.
42. Favre R., San Roman J. De Castro, The Arch: Enduring and Endaring. *Proceedings of the Third International Conference on Arch Bridge*. 19–21, Sept., Parie's France. 2001; 3–16.
43. Myroll F., Dibiagio E. Instrumentation for Monitoring the Skarnsunder Cable-stayed Bridge. *In: Jon Krokedorg, ed. Proceedings of the Third Symposium on Strait Crossing*. Rotterdam. 1994; 207-21.
44. Muria Vila D., Gomez R., King C.D. Dynamic Structural Properties of Cable Stayed Tam Pico Bridge. *Journal of Structural Engineering*. ASCE. 1991; 117(11): 3396–3416. [https://doi.org/10.1061/\(ASCE\)0733-9445\(1991\)117:11\(3396\)](https://doi.org/10.1061/(ASCE)0733-9445(1991)117:11(3396)).
45. Wace AJB. Excavations at Mycenae: IX. The Tholos Tombs. *Annual of the British School at Athens*. 1923; (25): 283–402.
46. Boyd TD. The Arch and the Vault in Greek Architecture. *American Journal of Archaeology*. 1978; 82(1): 83–100.
47. Pont dell'Abbadia [DB]. *Structurae.Science and Technology*, 2006, 32 (1): 124–126.
48. Galliazzo Vittorio. *Iponti romani: Catalogue generale*. Vol.2. Treviso: Edizioni Canova; 1994.
49. Colin O'Connor. *Roman Bridges* (First Edition). London: Cambridge University Press; 1993.
50. Troyano LF. *Atlante Storico University Dei Ponti*. Palermo: Dario Flaccovio Editore; 2006.
51. Gorazd H. Schönheit und Konstruktion der zerstorten Alten Brücke über die Neretva in Mostar (1566–1993). *Beton-und Stahlbetonbau*. 1996; 19(1): 18–20.
52. Wang Guoding, Zhong Shengbin. *Arch Bridge*. China communication press; 1997.
53. Chen Z, Zhouj J, Tse KT. et al. Alignment control for a long span urban rail-transit cable-stayed bridge considering dynamic train loads. *Sci. China Technol. Sci*. 2016. 59, 1759–1770. Available from: <https://doi.org/10.1007/s11431-016-0330-1>

INFORMATION ABOUT THE AUTHORS

Luojin Cao – engineer, senior engineer, College of Civil and Transportation Engineering, Shenzhen University, Shenzhen, Guangdong 518060, China, 281853271@qq.com

Nianqin Liu – engineer, senior engineer, Shenzhen Bridge Design and Research Institute Co., LTD., Shenzhen, Guangdong 518043, China, 40425988@qq.com

Xiangyu Li – engineer, senior engineer, Shenzhen College of international Education, Shenzhen, Guangdong 518110, China, katherineli.0207@gmail.com

Wenming Que – engineer, senior engineer, Shenzhen Bridge Design and Research Institute Co., LTD., Shenzhen, Guangdong 518043, China, 1290701515@qq.com

Yong Li – Dr. Sci. (Eng.), professor, College of Civil and Transportation Engineering, Shenzhen University, Shenzhen, Guangdong 518060, China, Liy2000@163.com

CONTRIBUTION OF THE AUTHORS

The authors contributed equally to this article.

The authors declare no conflicts of interests.

The article was submitted 15.07.2022; approved after reviewing 19.08.2022; accepted for publication 30.08.2022.